ε Aurigae—An Overview of the 2009–2011 Eclipse Campaign Results

Robert E. Stencel
University of Denver, Department of Physics and Astronomy, 2112 E. Wesley Avenue, Denver, CO 80208; rstencel@du.edu

Received March 19, 2012; revised May 30, 2012; accepted June 19, 2012

Abstract Evidence is provided from the array of observations amassed during the recent eclipse, that defines the enigmatic binary ε Aurigae as comprised of an unstable F0-1 Iab star, in orbit around a comparable mass upper main sequence star (or stars) enshrouded in a disk resulting from F star mass loss. In this picture, the F star may be undergoing rapid evolutionary changes, and the recent 67-day primary quasi-period may make it suitable for asteroseismic studies. The hidden star(s) may have gained mass from the F star, and the disk itself provides opportunities for study of accretion, dust evolution and dynamics.

1. Introduction

During the 20th century, the bright star ε Aurigae confounded astronomers because the visible member of this single-lined spectroscopic binary star appeared to be a massive, F-type supergiant star, with an equally-massive but invisible companion (Guinan and deWarf 2002). Unimpeachable evidence for the eclipsing object, a disk in transit, was obtained with interferometric imaging during the 2009–2010 eclipse (Kloppenborg *et al.* 2010), building on the infrared detection of same by Backman *et al.* (1984). Hoard *et al.* (2010), and previous authors, argued that the F star is in a volatile, reduced mass, post-Asymptotic Giant Branch (AGB) evoutionary phase, with the companion being a disk-enshrouded B-type main sequence star—possibly now the more massive object in the system. Resolution of the masses and evolutionary state of stars in this system is a primary motivator for the recent eclipse campaign, results of which are summarized in this paper. This article is part of a group of articles collected in the *Journal of the AAVSO*, intended to document results of an international effort to collect high quality observations of the ε Aur system during its 2009–2011 eclipse. Those reports provide details for each facet, but here we summarize some of the important findings, in relation to findings recognized as a result of the studies of previous eclipses.

2. Results

As discussed by Jeff Hopkins (2012), photometric V-band timings of the latest eclipse are as follows:

First contact:	RJD 55070	2009 August 16
"Second" contact:	RJD 55250	2010 February 22
Mid-eclipse:	RJD 55400	2010 July 22
"Third" contact:	RJD 55620	2011 February 27
Fourth contact:	RJD 55800	2011 August 26

where RJD = JD−2,400,000 and the uncertainty in timings is at least one to two weeks. The notion of contact times historically refers to tangent crossings between objects that appear circular in projection, but with a ellipsoidal disk shape involved, the normal meanings of second and third contacts are changed. Also, these timings are complicated by persistent ~0.1 magnitude light variations on a quasi-period of 67 days (Kim 2008). Spectroscopic evidence suggests that disk material encroached on the line of sight months prior to photometric first contact (for example, in K I 7699A—see Leadbeater *et al.*, this issue), or even years prior (Hα, see Chadima *et al.* 2011). Spectroscopic fourth contact was recently announced by observer Thierry Garrell who reported excess blue-shifted Hα and Na D-line absorption disappeared, circa RJD 55950 (2012 January 25).

The eclipsing object is a large, 550K flattened structure, based on recent infrared photometry and imaging. Although speculated to be a "swarm of meteors" by Hans Ludendorff early in the 20th century, the first photometric evidence for the eclipsing object was provided by Mitchell (1964) with nine-color photometry, who claimed a 500K excess, with a projected linear size of 50AU! Later, Backman *et al.* (1984) observed ε Aur entering eclipse and confirmed the result, reporting a 500K blackbody, with an apparent size of 8×10^{-16} ster-radians. At the reference distance of 650 pc, this translates to an area of 14 square-AU.

See Ed. comment on last page

The eclipsing object is disk shaped as seen in the near-IR. Thanks to remarkable progress in interferometric imaging over the past decade, it was possible in autumn 2009, during ingress, to detect the shadow of the disk crossing the face of the F star (Figure 1), using the MIRC beam combiner at the Center for High Angular Resolution Astronomy (CHARA) Array of telescopes atop Mt. Wilson, California (Kloppenborg 2010). More about this below.

The neutral potassium line at 7699Å reappeared and showed velocity shifts that associate it with the disk and its rotation. Originally reported by Lambert and Sawyer (1987), extensive monitoring by Robin Leadbeater (reported in this issue) showed a repeat of the phenomenon, demonstrating disk rotation and showing stepwise changes in the added equivalent width of the line, suggestive of disk substructure (Leadbeater and Stencel 2010). Subsequent study of spectra reveals a number of lines with this behavior (see Leadbeater *et al.* 2012; Schanne *et al.* 2012; Griffin and Stencel 2012).

The only molecule detected in ε Aur, so far, is transient carbon monoxide. This were originally reported by Hinkle and Simon (1987), and shown by Stencel *et al.* (2011) to reappear again after mid-eclipse, using both moderate resolution IRTF+SpeX and high dispersion Gemini North Near-IR Spectrometer (GNIRS) spectra. The data do not clearly confirm the low isotopic $^{12}C/^{13}C$ ratio ~10 (compared to the solar value, 89). The overlap of a Pfund series line of hydrogen atop the ^{13}CO bandhead demands post-eclipse observations where the CO contribution is removed, allowing disentanglement of the relative contribution. See Figures 2a and 2b. A less extreme $^{12}C/^{13}C$ ratio reduces the evidence for the F star being a lower mass, post-AGB star.

For the first time, transient He I 10830Å absorption was detected, and it strengthened around mid-eclipse (Stencel *et al.* 2011, using NASA's IRTF+SpeX instrument; see Figure 3). This line arises from a 19.8 eV level and suggests a high temperature central region in the disk. This is consistent with accretion onto a B0-B5 central star (Pequette *et al.* 2011).

Infrared monitoring confirmed the prediction by Takeuti (1986) that the side of the disk facing the F star is heated to 1100K (Hoard *et al.* 2012), in contrast to the 550K side facing away from the F star. Among the implications of this are that the binary separation might be evaluated, independent of the uncertain distance, and this degree of heating is related to the material properties of the dust in the disk.

A series of three in-eclipse observations of the the far-ultraviolet spectrum of ε Aur were obtained with the Cosmic Origins Spectrograph (COS) on Hubble Space Telescope (Howell *et al.* 2011), and it was found that the continuum output is somewhat eclipsed. The far-UV emission lines show evidence for a P Cygni-like outflow (Figure 4). Both facts point to surface activity of the F star, although contributions from the disk central regions cannot be ruled out.

Attempts to observe solid state spectral features (ices, PAHs, or 10-micron silicates) failed to detect any. Instruments involved included SpeX and BASS at NASA's IRTF, plus MIRAC at Mount Hopkins (see Stencel *et al.* 2011). The broadband infrared excess, combined with lack of spectral features, argues that the dust is comprised of large particles (greater than ~1 micron size). Kopal (1954) concluded similarly when studying the similarity of eclipse depth at many optical wavelengths—the eclipse is "gray" due to large particle sizes, much greater than the wavelengths involved. As noted above, eclipse depth departure from grayness is seen at wavelengths longer than several microns and in the ultraviolet, and these may provide useful constraints on particle size and type.

Photometric monitoring shows persistence of ~0.1 magnitude variations with a quasi-period of ~67 days (Kim 2008), both in and out of eclipse (Figure 5, and see Hopkins (2012)). These have been associated with F star oscillations and perhaps wind events (see Griffin and Stencel 2012).

3. System parameters

Among the generally agreed system parameters are the eclipse period, 9890±2 days, and the mass function in this single line spectroscopic binary, f(M) = 2.51±0.12 (Stefanik *et al.* 2010). System inclination seems securely established at very close to 90 degrees, based on interferometric images showing the disk eclipsing the primary star (Kloppenborg 2010). Given these parameters, possible solutions for the mass ratio (q) include the "high mass" case, q~1.1 (sum of masses, M+m~25 $M_{\odot}$, and semi-major axis, a~25AU) and the "low mass" case, q~0.5 (M+m~9 $M_{\odot}$, a~18AU), where M is the F star mass, and m refers to the mass of the secondary object – assumed to be star star inside the disk, and where a is the semi-major axis of the orbit. Astrometric solutions for both extremes have been published (Strand 1959; van de Kamp 1978). Work is underway to include interferometric results as a new constraint on combined astrometric and photometric solutions (Kloppenborg 2012), which favors the higher mass solution.

What constraints do we have on the *mass (M) of the primary star*? Classically, the spectral type of the primary star has been classified as an F0 Ia star (7500K). Yellow supergiant stars have cataloged masses of 12 $M_{\odot}$ and absolute magnitude, M_V=–6.6 (see, for example, Straizys and Kuriliene 1981). The historic q=1 solution for this single lined spectroscopic binary immediately called into question how a high mass companion could remain invisible outside of the eclipses it causes (Struve and Elvey 1930). Using the apparent magnitude, V=3.05 and the reddening, A_V=0.3, the implied distance is 740 pc (about 20% larger than that used by Kloppenborg (2010) based on the first Hipparcos parallax). From this, the implied luminosity is 3.7×10^4 $L_{\odot}$, and the implied radius is 115 $R_{\odot}$—larger than most Cepheids! At 740 pc, the angular diameter would be 1.5 milli-arcsec (hereafter, mas), at least 0.5 mas smaller than recent interferometric determinations (2.27 mas, K-band, Stencel *et al.* 2008). This requires the star to either have unusual limb darkening, or perhaps not be as distant as 740 pc. Formally, a 2.1 mas V-band uniform disk diameter indicates a distance of 650 pc.

An interesting constraint on binary separation can be deduced from recent thermal IR data, which shows that the portion of the disk nearest the F star rises to ~1100K (Stencel *et al.* 2011; Hoard *et al.* 2012). This equilibrium temperature for dust particles, with low albedo (0.3 to zero), implies a separation from the 7500K F0 star of 9 to 12 AU. For a disk radius of 4 to 5AU (see Kloppenborg 2010), the implied binary separation is 13 to 17 AU, which is more consistent with the q=0.5 solution. The sum of masses in this case ranges from 3 to 7 $M_{\odot}$. However, a distance of 1kpc distance, for example, requires a wider separation (25AU) to yield the same disk temperature, in a q=1 binary where the sum of masses would be 25 $M_{\odot}$.

In terms of resolving the ambiguity in distance and masses, two developments

deserve mention. Dissertation work by Brian Kloppenborg, at the University of Denver at the time of this writing, combined astrometric, spectroscopic and interferometric constraints on the orbit absolute dimensions. This resulted in a solution that places the system at 737 ± 67 pc, with a separation of 25 AU and masses of M = 13 and m = 11 $M_{\odot}$. The interferometrically constrained disk diameter of 7.31 ± –0.66 AU refers to the optically thickest portions and hence a minimum disk size, relative to the larger sizes implied by spectroscopic constraints.

What other constraints are possible on the mass (m) of the secondary star? Disk rotation curves may be obtained from the optically thin neutral potassium lines at 7699Å (Lambert and Sawyer 1986; Leadbeater *et al.* 2012), seen only during eclipse phases, and arguably arising from extreme outer portions of the disk. Their measured disk rotation speed is ~35 ± –5 km/sec. Rotation curves from optically thicker metallic lines (for example, Ti II 4028Å) indicate the disk rotation speed is 42 ± –2 km/sec (Saito *et al.* 1987). Then, with a disk radius value, we can determine a Keplerian rotation period at these speeds. Interferometric images were fitted by Kloppenborg (2010) with a 3.8 AU elliptical semi-major axis, assuming a 625 pc distance. Said rotation speeds (35, 42 km/sec) have implied circumferential rotation rates of 3.25 and 2.70 years, respectively, implying a central mass of 5.2 to 7.5 $M_{\odot}$. Saito *et al.* (1987) using eclipse timing arguments deduced that m < 5.3 $M_{\odot}$, whereas Lambert and Sawyer (1986) deduced m = 3 to 6 $M_{\odot}$ from their neutral potassium line velocity as a measure of disk rotation. These results strongly suggest the secondary star mass, m, is close to 4 to 6 $M_{\odot}$, comparable to that of a main sequence, B-type star. However, with a larger distance (737 pc) and using an optically thin disk radius (10 AU), these orbital speeds are consistent with a larger secondary mass (m = 11 $M_{\odot}$).

Another constraint on the mass of the secondary can be inferred from observed disk dust and gas scale heights. As shown by VEGA+CHARA observations (Mourard *et al.* 2012), the eclipse in Hα is total in comparison to the partial eclipse seen in the near-IR with the Michigan InfraRed beam Combiner (MIRC) at CHARA—that is, the hydrogen gas extends at least a full F star diameter above and below the disk plane. For strictly thermal dispersion of material, the scale height (H) to disk radius (R_D) ratio equals the sound speed-to-orbital velocity ratio, which is:

$$[H/R_D] = [(\gamma kT/\mu)/(Gm/R_D)]^{1/2} \quad (1)$$

(see Lissauer *et al.* 1996), where γ is the ratio of specific heats (5/3 for ideal gases), μ is the atomic mass and m is the central star mass. Tables and Figures in Lissauer *et al.* illustrate that the observed thickness is several times the scale height. The observed ratio of the minimum VEGA-observed thickness of gas disk (2.1 milli-arcsec, mas) relative to the estimated optically thick disk radius (8.92 mas – Kloppenborg 2012), is 0.24, suggesting a scale height to disk radius

ratio of 0.12 to 0.08. For the Hipparcos reference distance of 650 pc, the implied optically thick disk radius is 5.8 AU. Given the range of disk temperatures, 550 to 1100K, the thermal speed of hydrogen atoms ranges from 2.8 to 3.9 km/sec, and we deduce the quantity $(Gm/R)^{1/2}$ to be less than or equal to 35 km/sec, or implying again that the secondary star mass, m, is less than or equal to 10.7 $M_{\odot}$. For the larger distance estimate, 1 kpc, the implied disk radius becomes 8.9 AU and the disk temperatures result in a maximum mass of 16.5 $M_{\odot}$. In the absence of dynamical stirring, these masses are an upper limit, as the disk's hydrogen atmosphere could be thicker. Higher gas temperatures and/or a thicker disk scale height both point to a lower secondary mass. If the optically thin disk radius is larger than implied by the photometric eclipse duration, the resultant mass could be larger.

Are there any additional distance-independent discriminators? One might be the Eddington limit on luminosity, which is classically computed to be:

$$L_{Edd} / L_{\odot} = 3.8 \times 10^4 \, M / M_{\odot}. \quad (2)$$

For the two solutions offered, m = 3 to 4 and m = 15 to 25 $M_{\odot}$, the respective Eddington luminosities are $1.1 - 1.5 \times 10^5 L_{\odot}$ versus $5 - 9.5 \times 10^5 L_{\odot}$. Both ranges exceed the upper estimates for $L/L_{\odot}$. Other distance-independent means of establishing binary star parameters are needed.

3.1. Nature of the disk

Kloppenborg (2010) estimated that the disk fitted semi-major axis is 6.10 mas, meaning the full major axis is 12.2 mas or ~5.8 times F star diameter (2.1 mas). Given the reported 0.62 mas E-W motion per month during ingress (plus a N-S component 0.34 mas/month, for a net motion of 0.72 mas/month), and a 2.1 mas uniform disk diameter star, it should take ~2.9 months for a given point in the disk to move across the F star disk, assuming uniform motion, and ~18 months to have the entire disk move past, which is close to the observed first to third contact eclipse duration. The ellipse model devised during ingress was poorly constrained, dictated mainly by the expected length of eclipse. Afterwards, we obtained the complete light curve (Figure 5) and the first to fourth contact length in days is of order RJD 5800–5060 = 740 days, or ~24 months, and larger still in spectroscopic terms, suggesting the disk is larger than originally estimated and/or the relative velocities are varying (slowing, post-periastron).

Evidence exists that the disk is structured and asymmetric. There has been outstanding spectroscopic monitoring of Hα by Mauclaire *et al.* (2012) and of K I 7699Å by Leadbeater *et al.* (2012) and blue spectroscopic features by Griffin and Stencel (2012), reported in this issue and elsewhere, indicating an extended, asymmetric spectroscopic signature of the disk. The Hα equivalent width changes versus time suggest a compact ring may contribute to late phases

of ingress (RJD 55150–55250), while the disk main body is seen during totality (with a possible mid-eclipse decline circa RJD 55450, perhaps due to ionization related to the appearance of He I 10830Å (Stencel *et al.* 2011)). A more diffuse following ring associates with egress, but lasting past nominal fourth contact (RJD 55800) with excess Hα absorption still present in early 2012, a good 150 days past fourth contact. Similarly, the neutral potassium monitoring has been interpreted to show stepwise changes in equivalent width related to internal ring structure (Leadbeater and Stencel, 2010). These were labeled as rings A through F. Rings D and E might contribute to the late ingress Hα behavior, while rings D-A associate with egress phenomena. As reported elsewhere, however, the relationship between the dust and gas components is only just being revealed by spectro-interferometry obtained with the VEGA instrument at the CHARA Array (Mourard *et al.* 2012).

Additional suggestions of an ionizing photon induced shock in the ingress side of the disk has been made by Saito *et al.* (1987). Similarly, a matter transfer stream impacting the egress side of the disk had been advanced by Struve and colleagues early on, and something to this effect was seen again in blue region spectra reported by Griffin and Stencel (2012). Finally, the out of eclipse photometric variations are consistent with surface phenomena driven mass loss episodes from the F star that contribute to a stellar wind, asymmetrically shaped toward the center of mass and ionized by UV light scattered away from the source internal to the disk (Figure 6).

3.2. Dust scattering

The composition of the disk is of interest because determining dust size would provide evidence for the age of the object and the degree to which planetessimal formation may have occurred in the disk. Kopal (1954) noted the wavelength-independence of eclipse depths and concluded that large grains must be present with multi-micron sizes, much greater than optical wavelengths. However, observations to date have not detected any typical spectroscopic bands due to solids, such as ice (3 microns), PAHs, or 10-micron silicates (Stencel *et al.* 2011). An estimate for disk mass can be made, based on the far IR/sub-mm fluxes reported by Hoard *et al.* (2012):

$$M(\text{dust}) = F\nu\,\lambda^2\,d^2/(2\,k\,T_{\text{dust}}\,\kappa_\nu) \qquad (3)$$

where $F\nu$ (250 microns) = 57 mJy = 3×10^{-22} W/cm^2/micron. Using 650 pc as the distance, a dust temperature of 550K and a mass absorption coefficient, $\kappa_\nu = 3$ cm^2/gm (Jura *et al.* 2001), we deduce a dust mass of 1.2×10^{31} gm or nearly 6 Jupiter masses. This seems too large if the gas to dust ratio is ~100, because the disk mass would be dynamically significant in the system. Disk volume (Kloppenborg 2010) and deduced densities (Hinkle and Simon 1987) argue for a lower dust mass, roughly an Earth-mass. Dust opacity based on

sub-mm disk studies suggests that mass absorption coefficients are not well determined. Further work is needed to better characterize the material in the ε Aurigae disk (see Pearson and Stencel 2012).

Another avenue for exploring the disk content involves polarimetry. Broadband polarimetric studies have been reported by Kemp *et al.* (1986) and by Cole (2012). These show an out of eclipse baseline value in photometric V band of 2.0 percent, presumed to be interstellar, but growing and varying during eclipse to 2.4 percent. The substructure of V-band polarization during eclipse does not simply correlate with photometric changes. Kemp *et al.* (1986) correctly deduced the position angle of the eclipsing disk decades prior to the interferometric imaging of it. Recently, line polarization monitoring has become possible, greatly increasing insight into disk and star phenomena, and greatly complicating the analysis (see Geise *et al.* 2012).

One more line of evidence to be explored involves a difference between eclipse behavior among red wavelength lines like Hα and K I 7699Å, and blue wavelength lines like Fe I 3920Å and others. The former show equivalent width variation due to the eclipse, but remain substantially enhanced around mid-eclipse, while the bluer lines have equivalent width excess that nearly vanishes at mid-eclipse and then return strongly during late eclipse. This is to say that the line depth changes are less in the blue regions compared to the red regions, suggestive of particle sizes dominated by the greater than micron scale.

4. Archives

Table 1 lists observations that this author proposed and conducted, many of which will appear in public data archives maintained by the institutions involved. The AAVSO provides a comprehensive photometry archive. There are a number of spectroscopic data sources that might not be fully reflected in this report, but well worth the mention. In addition to the careful digitization by Elizabeth Griffin, of Mt. Wilson and DAO photographic spectra (plus new digital observations), additional modern high dispersion digital spectra were obtained regularly during eclipse by Hideyuki Izumiura at Okayama Observatory, by William Ketzeback and collaborators at Apache Point Observatory (see Barentine *et al.* 2012), by Nadine Manset and collaborators at CFHT (see Geise *et al.* 2012), by John Martin at the University of Illinois, Springfield, Observatory, by Nancy Morrison at the University of Toledo Ritter Observatory, by Ulisse Munari and collaborators at Asiago Observatory, by Klaus Strassmeier and collaborators (Astronomical Institute at Potsdam) STELLA telescope at IAC (see Schanne *et al.* 2012), and several others. Ideally, these data archives can be maintained by their originators and made available to interested researchers. This author would be happy to try to help coordinate analysis efforts.

5. Conclusions

Clarification of the nature of the eclipsing object in ε Aur will stand as one of the major achievements of this eclipse cycle. While the eclipse has brought attention to the study of ε Aur and its mysteries, we now have entered the long inter-eclipse period, prior to the start of the next eclipse circa 2036. Current orbital elements (Stefanik *et al.* 2010) predict key times that should be of interest to observers: the F star reaches maximum blue shift circa autumn 2017 (and it reached maximum redshift during autumn 2006). Eclipse of the disk by the F star is anticipated during 2020 and this should be detectable in the infrared, insofar as the observational capability exists then. There is merit in photometric monitoring of out of eclipse behavior, although the characteristic behavior (67-day quasi-period plus overtones and evolution) seems established (for example, Kim (2008) and Kloppenborg (2012)). The AAVSO's photometric data archive (www.aavso.org) provides an excellent resource. Nonetheless, with robotic telescopes and dedicated persons, the slow changes in this system can yet be followed during this newest orbital cycle.

6. Acknowledgments

There are many, many people to thank for help in this overall effort, making coverage of the recent eclipse the most complete in human history. Without Jeff Hopkins' and Lou Boyd's dedication to long term photometry, we would have a much sparser dataset. My thanks to Hal McAlister for accepting my proposals to use the CHARA Array for interferometric study of the eclipse, and to John Monnier for access to the MIRC instrument that made the imaging possible. Many facets of the work presented here were facilitated by Brian Kloppenborg and his amazing computer skills. I am grateful to Aaron Price, Rebecca Turner, and Arne Henden at AAVSO for their efforts with the Citizen Sky observer campaign that enriched the data archives with thousands of new measures, all carefully archived. Additional spectroscopic monitoring was contributed by Robin Leadbeater, Thierry Garrel, Christian Buil, Elizabeth Griffin, and many others. Key collaborators on HST COS and Spitzer/IRAC data acquisition included Steve Howell and Donald Hoard, with excellent advice received from COS team members Stephane Beland, Jim Green, Steven Penton, and others. Collaborators obtaining and reducing Gemini North GNIRS data were Tom Geballe and Rachel Mason. Helpful comments on this paper from an anonymous referee are appreciated. My participation was supported in part by the bequest of William Herschel Womble in support of Astronomy at the University of Denver, for which I am extremely grateful (as the project would not have been possible otherwise), along with an NSF-RAPID grant, AST 10-16678 to the University of Denver, organized by the prescient program director Donald Terndrup, who deserves public thanks for recognizing the singular opportunity afforded by ε Aur.

References

Backman, D. E., Becklin, E. E., Cruikshank, D. P., Joyce, R. R., Simon, T., and Tokunaga, A. 1984, *Astrophys. J.,* **284**, 799.

Barentine, J., *et al.* 2012, *Bull. Amer. Astron. Soc.*, **44**, 433.312.

Chadima, P., *et al.* 2011, *Astron. Astrophys.*, **530A**, 146.

Cole, G. 2012, *J. Amer. Assoc. Var. Star Obs.,* **40**, in press.

Geise, K., Stencel, R., Manset, N., Harrington, D. and Kuhn, J. 2012, *J. Amer. Assoc. Var. Star Obs.,* submitted.

Griffin, R. E. M. G., and Stencel, R. 2012, *J. Amer. Assoc. Var. Star Obs.,* **40**, in press, and *Publ. Astron. Soc. Pacifc*, submitted.

Guinan, E., and Dewarf, L. 2002, in *Exotic Stars as Challenges to Evolution*, eds. C. A. Tout and W. Van Hamme, ASP Conf. Ser., 279, Astron. Soc. Pacific, San Francisco, 121.

Hinkle, K., and Simon, T. 1987, *Astrophys. J.,* **315**, 296.

Hoard, D., Howell, S., and Stencel, R. 2010, *Astrophys. J.,* **714**, 549.

Hoard, D., Ladjal, D., Stencel, R., and Howell, S. 2012, *Astrophys. J., Lett. Ed.*, **748**, L28.

Hopkins, J., 2012, *J. Amer. Assoc. Var. Star Obs.*,**40**, in press.

Howell, S., Hoard, D., and Stencel, R. 2011, Bull. Amer. Astron. Soc., **43**, 257.07.

Jura, M., Webb, R. A., and Kahane, C. 2001, *Astrophys. J., Lett. Ed.*, **550**, L71.

Kemp, J. C., Henson, G. D., Kraus, D., Beardsley, I., Carroll, L., Ake, T., Simon, T., and Collins, G. 1986, *Astrophys. J., Lett. Ed.*, **300**, L11.

Kim, H. 2008, *J. Astron. Space Sci.*, **25**, 1.

Kloppenborg, B. 2012, Ph.D. thesis, University of Denver.

Kloppenborg, B., *et al.* 2010, *Nature*, **464**, 870.

Kopal, Z. 1954, *Observatory*, **74**, 14.

Lambert, D., and Sawyer, S. 1986, *Publ. Astron. Soc. Pacific*, **98**, 389.

Leadbeater, R., and Stencel, R. 2010, http://arxiv.org/abs/1003.3617.

Leadbeater, R., *et al.* 2012, *J. Amer. Assoc. Var. Star Obs.,* submitted.

Lissauer, J., Wolk, S., Griffith, C., and Backman, D. 1996, *Astrophys. J.*, **465**, 371.

Mauclaire, B., Buil, C., Garrel, T., Leadbeater, R., and Lopez, A. 2012, *J. Amer. Assoc. Var. Star Obs.,* **40**, in press.

Mourard, D., *et al.* 2012, *Astron. Astrophys.*, in press.

Pearson, R., and Stencel, R. 2012, *J. Amer. Assoc. Var. Star Obs.,* **40**, in press.

Pequette, N., Stencel, R., and Whitney, B. 2011, *Bull. Amer. Astron. Soc.*, **43**, 225.05.

Saito, M., Kawabata, S., Saijo, K., and Sato, H. 1987, *Publ. Astron.*, **39**, 135.

Schanne, L., Strassmeier, K., Weber, M., Leadbeater, R., and Stencel, R. 2012, *J. Amer. Assoc. Var. Star Obs.,* **40**, submitted.

Stefanik, R., Torres, G., Lovegrove, J., Pera, V., Latham, D., Zajac, J., and Mazeh, T. 2010, *Astron. J.*, **139**, 1254.

Stencel, R. E., Creech-Eakman, M., Hart, A., Hopkins, J. L., Kloppenborg, B. K., and Mais, D. E. 2008, *Astrophys. J., Lett. Ed.*, **689**, L137.
Stencel, R., *et al.* 2011, *Astron. J.*, **142**, 174.
Straizys, V., and Kuriliene, G. 1981, *Astrophys. Space Sci.*, **80**, 353.
Strand, K. 1959, *Astron. J.*, **64**, 346.
Struve, O., and Elvey, C. 1930, *Astrophys. J.*, **71**, 136,
Takeuti, M. 1986, *Astrophys. Space Sci.*, **121**, 127.
van de Kamp, P. 1978, *Astron. J.*, **83**, 975.

Table 1. Selected new observations of ε Aur during eclipse, 2009–2011.

*RJD**	*Calendar Date*	*Telescope*	*Mode*
55084	2009 Sep 10	IRTF/SpeX	1–5-micron med-res spectra
55139	2009 Nov 2–4	CHARA+MIRC	1.6-micron interferometric imaging
55140	2009 Nov 3	IRTF/SpeX	1–5-micron med-res spectra
55169	2009 Dec 2–4	CHARA+MIRC	1.6-micron interferometric imaging
55197	2010 Jan 1	MMTO/MIRAC	10-micron photometry/spectra
55245	2010 Feb 18	CHARA+MIRC	1.6-micron interferometric imaging
55250	2010 Feb 23	IRTF/SpeX	1–5-micron med-res spectra
55428	2010 Aug 19–21	CHARA+MIRC	1.6-micron interferometric imaging
55432	2010 Aug 24	IRTF/SpeX	1–5-micron med-res spectra
55441	2010 Sep 1	HST/COS	far-UV spectra
55462	2010 Sep 22–23	CHARA+MIRC	1.6-micron interferometric imaging
55467	2010 Sep 27	IRTF/SpeX	1–5-micron med-res spectra
55494	2010 Oct 24	MMTO/CLIO	JHKLM photometry
55495	2010 Oct 25–26	CHARA+MIRC	1.6-micron interferometric imaging
55499	2010 Oct 29	IRTF/SpeX	1–5-micron med-res spectra
55500	2010 Oct 29	Spitzer/IRAC	3.6 and 4.6-micron photometry
55513	2010 Nov 12	IRTF/SpeX	1–5-micron med-res spectra
55523	2010 Nov 22	Spitzer/IRAC	3.6 and 4.6-micron photometry
55537	2010 Dec 6	IRTF/SpeX	1–5-micron med-res spectra
55540	2010 Dec 9–10	CHARA+MIRC	1.6-micron interferometric imaging
55540	2010 Dec 9	HST/COS	2nd far-UV spectrum
55553	2010 Dec 22	MMTO/MIRAC	10-micron photometry/spectra
55559	2010 Dec 28/9	GNIRS SV	2.3-micron high-res CO spectra
55565	2011 Jan 04	GeminiN+GNIRS	2.3-micron high-res spectra
55567	2011 Jan 06	IRTF/SpeX	1–5-micron med-res spectra
55582	2011 Jan 19	CHARA+MIRC4T	1.6-micron interferometric imaging
55567	2011 Mar 3/4	IRTF+SpeX	attempt, 1–5-micron med-res spectra
55637	2011 Mar 17	HST+COS	1150–1800Å spectra (3rd epoch)
55637	2011 Mar 17/18	CHARA+CLIMB	3T interferometry
55649	2011 Mar 29	IRTF+SpeX	JTR, 1–5-micron med-res spectra

Table continued on next page

Table 1. Selected new observations of ε Aur during eclipse, 2009–2011, cont.

RJD[1]	Calendar Date	Telescope[2]	Mode
55650	2011 Mar 30	GeminiN+GNIRS	2.3-micron high-res spectra
55651	2011 Apr 1–5	CHARA+CLIMB	3T interferometry
55663	2011 Apr 12	IRAC	3.5 and 4.5-micron photometry
55663	2011 Apr 12	GeminiN+GNIRS	2.3-micron high-res spectra
55663	2011 Apr 12	Spitzer/IRAC	3.6 and 4.6-micron photometry
55678	2011 Apr 25	IRTF+MIRSI	10-micron photometry
55680	2011 Apr 29	Spitzer/IRAC	3.6 and 4.6-micron photometry
55814	2011 Sep 10	HSO–PACS	70, 110, 160-micron photometry
55824	2011 Sep 18	CHARA+MIRC6T	1.6-micron interferometric imaging
55826	2011 Sep 21	HSO–SPIRE	250, 350, 500-micron photometry
55830	2011 Sep 24	CHARA+MIRC6T	1.6-micron interferometric imaging
55830	2011 Sep 24	IRTF+SpeX	1–5-micron med-res spectra
55846	2011 Oct 10	CHARA+MIRC6T	1.6-micron interferometric imaging
55869	2011 Nov 03	CHARA+MIRC6T	1.6-micron interferometric imaging
55871	2011 Nov 05	MMT+MIRAC4	clouded out
55884	2011 Nov 17	Spitzer/IRAC	3.6 and 4.6-micron photometry
55894	2011 Nov 27	IRTF+SpeX	1–5-micron med-res spectra
55899	2011 Dec 02	Spitzer/IRAC	3.6 and 4.6-micron photometry
55913	2011 Dec 16	CHARA+MIRC	clouded out
55915	2011 Dec 18	IRTF+SpeX	1–5-micron med-res spectra

[*]*RJD = JD– 2400000.*

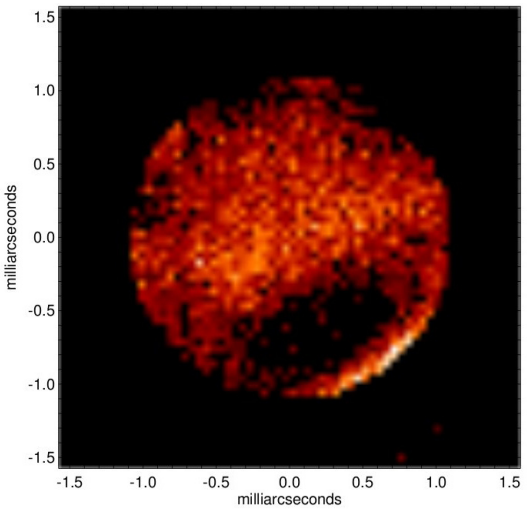

Figure 1. Historic first: the 1.6-micron wavelength image of ε Aur 2009 November 2 as initially processed by John Monnier, based on four telescope beam combination data acquired by MIRC at the CHARA Array. The scales are in milli-arcsecond units.

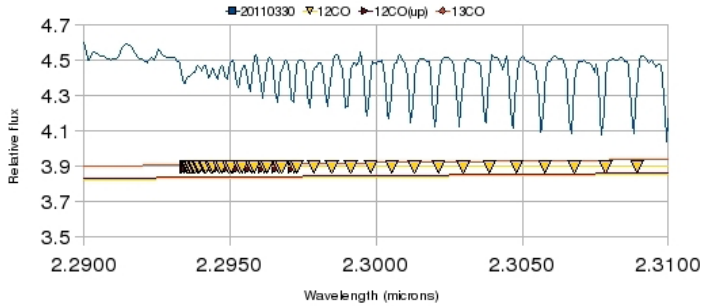

Figure 2a. A portion of the Gemini North GNIRS spectrum of ε Aur spanning the ^{12}CO (2-0) bandhead at 4360 cm-1 region (2.293 microns) showing spectral lines of ^{12}CO(2-0 up) and ^{12}CO(2-0 down), illustrating the GNIRS resolution capable of separating these contributions. The lines show a –25 km/sec systematic blueshift, characteristic of the disk at this epoch.

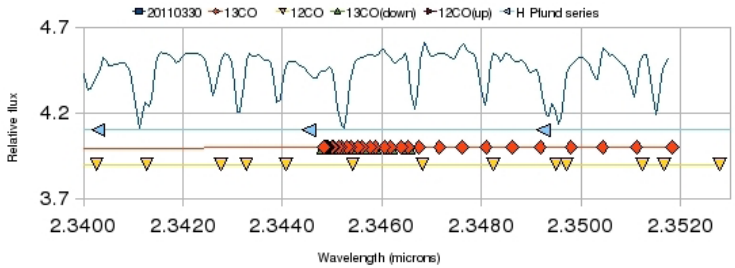

Figure 2b. A portion of the Gemini North GNIRS spectrum of ε Aur spanning the ^{13}CO (2-0) bandhead at 4265 cm-1 region (2.344 microns) showing spectral line positions of ^{13}CO(2-0), ^{12}CO(2-0), ^{12}CO (3-1) lines and hydrogen P_{fund} lines. Redshifted P_{fund} line absorption may account for some, or all, of the previously reported ^{13}CO bandhead near 2.345 microns.

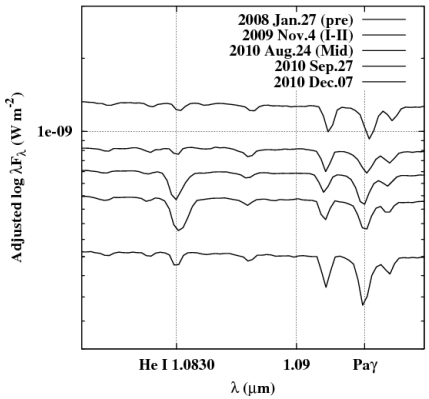

Figure 3. Time series of IRTF+SpeX data showing mid-eclipse appearance of He 10830Å.

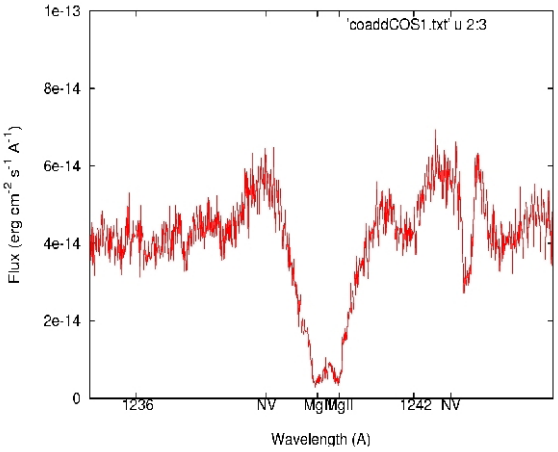

Figure 4a. HST/COS spectra of ε Aur. The strong UV Mg II doublet at 1240Å (1239.925, 1240.395) but lack of N V (1238.821, 1242.804). The line near 1243.3 could be N I.

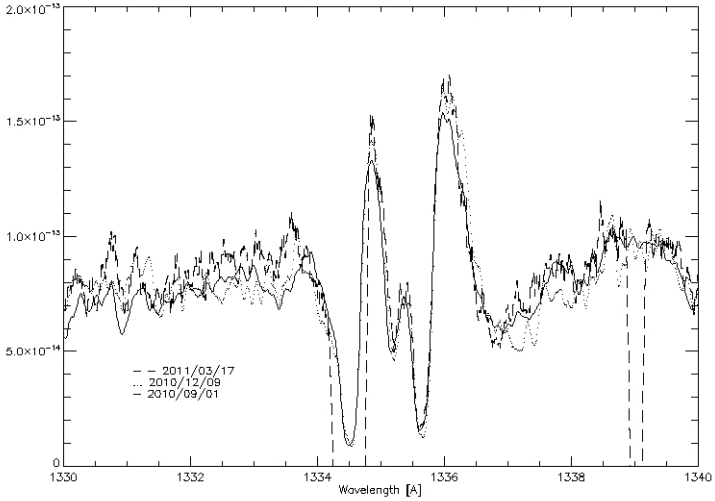

Figure 4b. C II profiles showing clear P Cygni outflow, unaffected by eclipse phase.

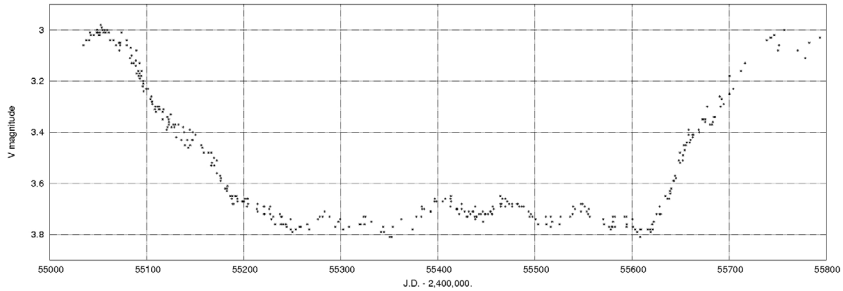

Figure 5. V magnitude record of the 2009–2011 eclipse of ε Aur as recorded by a variety of observers. See Stencel *et al.* (2011) for details.

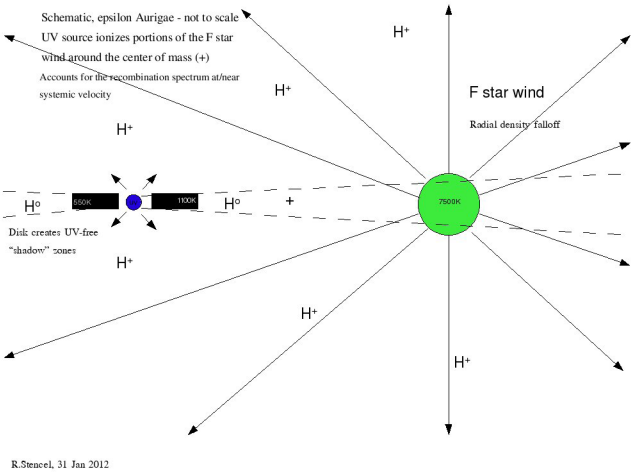

Figure6. Schematic model of ε Aur that incorporates F star wind focusing and ionization effects due to scattering of UV photons originating inside the dark disk. This model accounts for many of the newly observed spectroscopic and radial velocity details reported here and in related papers, and provides predictions for advanced high-resolution imaging in the future.

Ed. comment (see page 2): Confusing: if the disc is 50 AU, how can the disc area be 14 AU? Or do you mean the projected area?